Earth and Planetary Science Letters 400 (2014) 195–205

Contents lists available at ScienceDirect

Earth and Planetary Science Letters

www.elsevier.com/locate/epsl

Cosmogenic noble gas paleothermometry

Marissa M. Tremblay [a,b,*], David L. Shuster [a,b], Greg Balco [b]

[a] Department of Earth and Planetary Science, University of California, Berkeley, 307 McCone Hall #4767, Berkeley, CA 94720-4767, USA
[b] Berkeley Geochronology Center, 2455 Ridge Road, Berkeley, CA 94709, USA

ARTICLE INFO

Article history:
Received 30 March 2014
Received in revised form 22 May 2014
Accepted 23 May 2014
Available online 10 June 2014
Editor: T.M. Harrison

Keywords:
cosmogenic nuclide
noble gas
diffusion
paleoclimate
surface processes

ABSTRACT

We present a theoretical basis for reconstructing paleotemperatures from the open-system behavior of cosmogenic noble gases produced in minerals at Earth's surface. Experimentally-determined diffusion kinetics predicts diffusive loss of cosmogenic ^{3}He and ^{21}Ne from common minerals like quartz and feldspars at ambient temperatures; incomplete retention has also been observed empirically in field studies. We show that the theory of simultaneous production and diffusion that applies to radiogenic noble gases in minerals—the basis of thermochronology—can also be applied to cosmogenic noble gases to reconstruct past surface temperatures on Earth. We use published diffusion kinetics and production rates for ^{3}He in quartz and ^{21}Ne in orthoclase to demonstrate the resolving power of cosmogenic noble gas paleothermometry with respect to exposure duration, temperature, and diffusion domain size. Calculations indicate that, when paired with a quantitatively retained cosmogenic nuclide such as ^{21}Ne or ^{10}Be, observations of cosmogenic ^{3}He in quartz can constrain temperatures during surface exposure in polar and high altitude environments. Likewise, ^{21}Ne retention in feldspars is sensitive to temperatures at lower latitudes and elevations, expanding the potential geographic applicability of this technique to most latitudes. As an example, we present paired measurements of ^{3}He and ^{10}Be in quartz from a suite of Antarctic sandstone erratics to test whether the abundances of cosmogenic ^{3}He agree with what is predicted from first principles and laboratory-determined diffusion kinetics. We find that the amounts of cosmogenic ^{3}He present in these samples are consistent with the known mean annual temperature (MAT) for this region of Antarctica between −25 and −30 °C. These results demonstrate the method's ability to record paleotemperatures through geologic time.

1. Introduction

Reconstructing past surface temperatures from continental settings is important for understanding how climatic processes, such as glacial cycles, and tectonic processes, such as orogenic-driven elevation change, have shaped terrestrial environments and landforms. The most widely applied methods for reconstructing past surface temperatures on continents involve measuring stable isotopes of oxygen in carbonates or ice. However, in the case of carbonates, traditional stable isotope methods require that the oxygen isotopic composition of water from which carbonate formed is known, which is rarely the case (e.g. Eiler, 2011; Kim and O'Neil, 1997; Rowley and Garzione, 2007). In the past decade, measurements of multiply substituted isotopologues ("clumped isotopes") in carbonates have circumvented this limitation (Eiler, 2007; Ghosh et al., 2006). Nevertheless, temperatures calculated from carbonate clumped isotope measurements can be anomalously high (Quade et al., 2011) and vary as a function of seasonal parameters like precipitation (Peters et al., 2012) precluding simple interpretation in some cases. Leaf physiognomy (e.g. Forest et al., 1999; Gregory and McIntosh, 1996) and pollen distribution (e.g. Bartlein et al., 2011) have also been used to estimate terrestrial paleotemperatures. However, these bioclimatic proxies depend on numerous additional climate parameters, including precipitation, plant-available moisture, seasonality, and length of the growing season. All existing terrestrial paleotemperature proxies are limited by the abundance of specific minerals/fossils in the rock record and can suffer from poor preservation and diagenetic alteration (Eiler, 2011). Thus quantitative reconstruction of past terrestrial temperatures remains a major challenge despite the development of several paleotemperature proxies over the past few decades.

In this paper we describe a new paleotemperature proxy based on the open-system behavior of cosmogenic noble gases in common minerals. ^{3}He and ^{21}Ne were the first *in situ*-produced

* Corresponding author at: Department of Earth and Planetary Science, University of California, Berkeley, 307 McCone Hall #4767, Berkeley, CA 94720-4767, USA. Tel.: +1 603 203 4976.
E-mail addresses: mtremblay@berkeley.edu (M.M. Tremblay), dshuster@berkeley.edu (D.L. Shuster), balcs@bgc.org (G. Balco).

http://dx.doi.org/10.1016/j.epsl.2014.05.040
0012-821X/

cosmogenic nuclides to be unambiguously observed in terrestrial materials (Craig and Poreda, 1986; Kurz, 1986; Marti and Craig, 1987). Since then, measurements of cosmogenic nuclides in minerals have transformed how Earth surface processes are studied and quantified (Granger et al., 2013). ^{3}He and ^{21}Ne are particularly attractive for studying surface processes. Since ^{3}He and ^{21}Ne are both stable, they can be used to quantify exposure histories that are long relative to the half-lives of cosmogenic radionuclides like ^{10}Be and ^{26}Al. Cosmogenic ^{3}He and ^{21}Ne also have high production rates in terrestrial materials, minimizing the amount of material needed for analysis, and noble gas measurements are faster and cheaper than measurements of cosmogenic radionuclides by accelerator mass spectrometry. Cosmogenic ^{21}Ne in quartz, olivine, pyroxene, and amphibole and cosmogenic ^{3}He in the latter three phases have been extensively used to study geomorphic and geologic processes (e.g. review by Dunai, 2010). Empirical observations (Bruno et al., 1997; Cerling, 1990; Ivy-Ochs et al., 2007; Schäfer et al., 1999), and in some cases measured diffusion kinetics (Cherniak et al., 2014; Gourbet et al., 2012; Shuster and Farley, 2005; Trull et al., 1991), indicate that these cosmogenic noble gas–mineral pairs exhibit quantitative retention at Earth surface temperatures.

In contrast, cosmogenic ^{3}He and ^{21}Ne experience significant diffusive loss over geologic time at Earth's surface in quartz and feldspars, respectively. As a result, these cosmogenic noble gas–mineral pairs have been almost entirely avoided in surface process studies. Incomplete retention of cosmogenic ^{3}He was first inferred from comparisons of ^{3}He-based exposure ages with ^{10}Be or ^{26}Al ages from the same quartz samples. In diverse settings, the ^{3}He ages were systematically younger (Brook and Kurz, 1993; Brook et al., 1993; Cerling, 1990; Trull et al., 1995). Experimentally-determined diffusion kinetics of ^{3}He in quartz broadly agrees with these observations and indicates that significant proportions of ^{3}He can be lost from quartz over time, even at subzero temperatures (Shuster and Farley, 2005). Although one study showed that ^{3}He could be quantitatively retained in very large quartz grains with $<$100 ka of exposure in Antarctica (Brook et al., 1995), the only published cosmogenic ^{3}He–quartz measurements since the mid-1990s were used to screen for relatively old versus young erratics and sub-select samples for ^{10}Be analyses (Ackert Jr. et al., 2011). Observations of cosmogenic ^{21}Ne in feldspars (Bruno et al., 1997; Kober et al., 2005) and experimentally-determined diffusion kinetics of Ne (Gourbet et al., 2012) suggest that feldspars can also experience diffusive loss of cosmogenic ^{21}Ne at Earth's surface, depending on mineralogical composition. Sanidine, which apparently exhibits quantitative retention of ^{21}Ne (Gourbet et al., 2012; Kober et al., 2005), is the only feldspar that has been used to study surface processes (Ivy-Ochs et al., 2007; Kober et al., 2007).

Although avoided in cosmogenic nuclide studies, the open-system behavior of radiogenic noble gases has been extensively studied and utilized as a method for reconstructing thermal histories of minerals and rocks in the upper lithosphere (Harrison and Zeitler, 2005). Widely applied methods of noble gas thermochronology, such as the ^{40}Ar/^{39}Ar system in feldspars and the (U–Th)/He system in apatite and zircon, record both time, through the production of noble gas atoms via radioactive decay, and temperature, through their thermally-activated diffusive loss. In principle, cosmogenic noble gas–mineral pairs exhibiting open-system behavior also record the thermal histories of rocks that can be quantified using the same theoretical framework as radiogenic noble gases. Since cosmogenic nuclide production occurs almost entirely within the uppermost few meters of the Earth's surface, cosmogenic noble gas–mineral pairs ought to record thermal histories of local surface environments.

Here we present calculations to test whether the open-system behavior of cosmogenic ^{3}He in quartz and ^{21}Ne in feldspars can be used to quantify past temperatures at Earth's surface. We utilize published production rates and diffusion kinetics of these cosmogenic noble gas–mineral pairs, although future paleothermometry applications will warrant tighter constraints on both of these variables. We show that with relatively simple models based on first principles we can predict the observed abundances of cosmogenic ^{3}He in an example set of quartz samples from Antarctica with simple Holocene exposure histories. This work focuses on ^{3}He and ^{21}Ne in quartz and feldspars, respectively, but the theoretical framework presented here can be extended to any cosmogenic noble gas–mineral system and to other planetary bodies and higher temperature regimes (e.g. Shea et al., 2012; Shuster et al., 2010; Suavet et al., 2013). Further, this cosmogenic nuclide-based paleothermometer, which is characterized by fundamentally different principles and assumptions from preexisting paleotemperature proxies, may be particularly useful for studying surface processes where pre-existing proxies cannot be applied, or provide important tests for internal consistency in cases where they can.

2. Theoretical background

2.1. Simultaneous production and diffusion

The theory and mathematics describing the open-system behavior of noble gases in minerals have been extensively developed in the field of noble gas thermochronology; we present a brief review of fundamental concepts here. The concentration of a noble gas M simultaneously being produced and diffusing from a mineral changes as a function of time t according to:

$$\frac{\partial M}{\partial t} = \frac{D(T)}{a^2}\nabla^2 M + P_M \tag{1}$$

where D is diffusivity, ∇^2 is the second-order spatial derivative or Laplacian, a is the dimension of the diffusion domain, and P_M is the mineral-specific production rate of M. Eq. (1) requires that diffusion of noble gases in the mineral is Fickian (i.e., atoms move from regions of high to low concentration with a flux proportional to the concentration gradient) and isotropic. Published diffusion experiments suggest that these conditions are met for noble gas diffusion in quartz (Shuster and Farley, 2005) and orthoclase (Gourbet et al., 2012). Solutions to Eq. (1) must also satisfy the boundary condition that the concentration of M at a, the outer boundary of the diffusion domain, is zero. This condition is effectively valid for minerals when the diffusion domain is equivalent to the grain size, as diffusivities along grain boundaries are typically several orders of magnitude greater than within the mineral grains themselves (e.g. Dohmen and Milke, 2010), and the surrounding environment is nearly an infinite reservoir for rare nuclides. Abundances of cosmogenic ^{3}He in different grains sizes sharing a common exposure history indicate that the diffusion domain and grain size are equivalent for quartz (Brook et al., 1993). For thermally-activated diffusion of noble gases in minerals, a large body of research (e.g. review by Baxter, 2010) shows that the diffusivity D depends exponentially on temperature according to the Arrhenius relationship:

$$\frac{D(T)}{a^2} = \frac{D_0}{a^2}\exp\left(\frac{-E_a}{RT(T)}\right) \tag{2}$$

where D_0 is the diffusivity at infinite temperature, E_a is the activation energy, R is the gas constant and T is temperature. The diffusion parameters D_0 and E_a are specific to a particular noble gas–mineral pair and can be determined empirically via laboratory experiments. If both temperature (and therefore diffusivity) and the production rate remain constant through time, and if we assume the diffusion domain has a spherical geometry, Eq. (1) has the analytical solution described by Wolf et al. (1998):

$$M(t) = P_M \frac{a^2}{D}\left[\frac{1}{15} - \sum_{n=1}^{\infty} \frac{6}{\pi^4 n^4} \exp\left(-\pi^2 n^2 \frac{D}{a^2} t\right)\right] \quad (3)$$

The spherical geometry assumption is reasonable for most mineral grains with modest aspect ratios, as long as the surface area to volume ratio of the actual diffusion domain and the spherical approximation are equivalent (Farley et al., 2010; Meesters and Dunai, 2002). When temperature and/or production vary as a function of time, the analytic approach is no longer valid and a numerical solution is required. For calculations in this paper involving time-varying production rates, we implement the Crank–Nicholson finite-difference scheme described by Ketcham (2005) to discretize and solve Eq. (1).

2.2. Cosmogenic nuclide production

A fundamental difference between solutions to Eq. (1) for radiogenic and cosmogenic noble gases is the production term (for an extensive review of cosmogenic nuclide production, see Dunai, 2010; Gosse and Phillips, 2001). Cosmogenic nuclides are produced when high-energy cosmic-ray particles ultimately induce nuclear transmutations, typically spallation reactions, of target atoms in a mineral. Production rates depend on i) the flux and energy spectrum of incident particles, ii) the elemental composition of the target mineral, and iii) the cross-sections of relevant reactions. At typical Earth surface elevations, the flux of energetic particles is primarily controlled by an exponential dependence of production rate on the thickness of shielding mass (e.g., the overlying atmosphere and any additional shielding by rock or soil) above the sample (Lal, 1991). Given a mineral with uniform composition (e.g. quartz), however, the production ratio of two cosmogenic nuclides can only vary if both the relevant reaction cross-sections depend differently on particle energy and the energy spectrum of the cosmic-ray flux changes. Since cross-sections of most geologically relevant reactions have similar energy dependence, and since the energy spectrum of the cosmic-ray flux is nearly invariant at typical surface elevations, the production rate ratio of two nuclides in a particular target mineral is essentially constant over time regardless of the variation in absolute production rate due to surface erosion or deposition. In practice, nearly all surfaces on Earth are subject to either erosion or deposition, so incorporating the time-dependence of production in solutions to Eq. (1) will be important for reconstructing thermal histories from cosmogenic noble gases.

Apparent exposure ages can be determined from the concentration M and local production rate P_M of a cosmogenic noble gas exhibiting open-system behavior in a particular mineral (Eq. (1)). However, like open-system behavior of radiogenic noble gases, this apparent age has little significance by itself, providing only a lower bound on exposure age. Additional information is required to reconstruct a thermal history. In the simplest case of a single period of surface exposure with negligible erosion, this information can be obtained by pairing the partially-retained nuclide with one that is not subject to diffusive loss. Given knowledge of relevant production rates, the concentration of the quantitatively-retained nuclide establishes the exposure duration, and the concentration of the partially-retained nuclide becomes a function only of the integrated temperature over a sample's exposure. In the case of more complex exposure histories involving erosion and/or burial, changes in depth and production rate with time can be determined from the concentration–depth profile of one or paired measurements of two quantitatively retained cosmogenic nuclides (Jungers et al., 2013; Kober et al., 2007; Schaller et al., 2009). Thus we can use measurements of one or more quantitatively retained nuclides to independently determine both the time interval over which to solve Eq. (1) and how the production term evolves. Once the exposure history of the sample is known, the concentration of the partially-retained nuclide is directly related to the temperature experienced by the sample during that history.

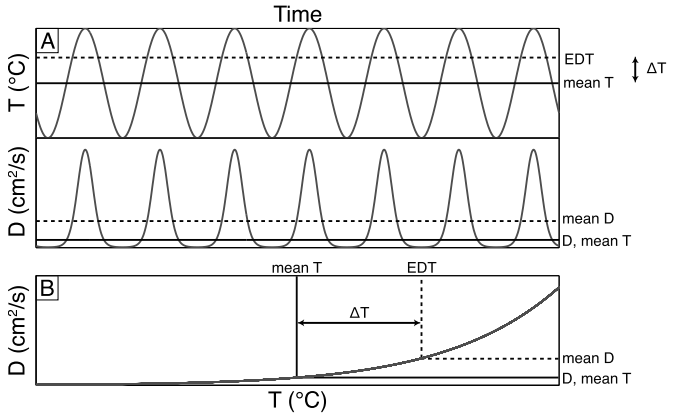

Fig. 1. Schematic illustration of ΔT, the difference between effective diffusion temperature (EDT) and mean temperature. The EDT is calculated from the mean diffusivity D experienced over the temperature function in (A), which will always be greater than or equal to the mean temperature since diffusivity is a nonlinear function of temperature (B).

2.3. Effects of surface temperature variability on cosmogenic noble gas diffusion

Rocks at Earth's surface experience temperature oscillations on daily, seasonal, and longer timescales. Because diffusion is a continuous process and a nonlinear function of temperature, these periodic surface temperature oscillations will influence the time-integrated thermal history that a cosmogenic noble gas–mineral pair records. We are ultimately interested in changes in mean ambient temperatures over geologic time. Therefore we need to account for the effects of periodic temperature variations on diffusivity in order to infer mean ambient temperatures from measurements of cosmogenic noble gases. This can be achieved by defining the effective diffusion temperature, or EDT, as the temperature corresponding to the mean diffusivity over a variable temperature function. Mathematically, the EDT can be written by transforming Eq. (2):

$$EDT = \frac{-E_a}{R}\left(\ln\left[\frac{1}{t}\int_0^t \exp\left(\frac{-E_a}{RT(t')}\right)dt'\right]\right)^{-1} \quad (4)$$

where t is the period of the temperature variation. This concept of an effective temperature has been previously defined and applied in the thermoluminescence literature (Christodoulides et al., 1971; Durrani et al., 1972). We use the term effective diffusion temperature here to emphasize that, given the same temperature function, the effective temperature of solid-state noble gas diffusion may not be the same as the effective temperature for another temperature-dependent process. Since diffusivity is a nonlinear function of temperature, the EDT will always be greater than or equal to the mean temperature of a given temperature function. To conceptualize this, Fig. 1 shows the relationship between temperature and diffusivity for a sinusoidal temperature function.

The difference between EDT and mean temperature (ΔT, Fig. 1) is a function of the mean temperature, amplitude of the temperature oscillation, and diffusion parameters used to calculate EDT with Eq. (4), but is independent of frequency for a one component temperature oscillation, as in Fig. 1. For a given mean temperature, ΔT increases with increasing amplitude. This means that rock samples at the surface experiencing the same mean temperature and exposure duration can have different EDTs and therefore observable differences in cosmogenic noble gas retention, such that

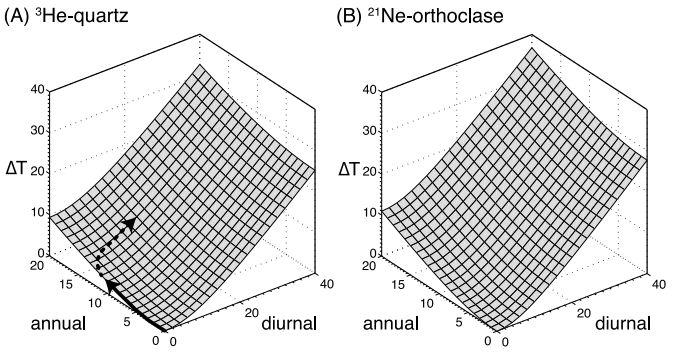

Fig. 2. ΔT, the difference between effective diffusion temperature (EDT) and mean temperature, as a function of the amplitudes of diurnal and annual temperature oscillations for a mean temperature of 0 °C, calculated according to Eq. (4). We show ΔT surfaces for both the ^{3}He–quartz (A) and ^{21}Ne–orthoclase (B) systems using the diffusion kinetics of Shuster and Farley (2005) and Gourbet et al. (2012), respectively. For higher mean temperatures, ΔT surfaces plot sub-parallel to and below the surface for 0 °C shown; the converse is true for lower mean temperatures. In (A), we show an example of how ΔT might evolve for a constant mean temperature as a sample approaches the surface due to erosion. Below ~14 cm, the ΔT experienced by a sample is primarily a function of the annual temperature oscillation and evolves along the solid arrow. Above ~14 cm, the amplitude of the annual temperature oscillation approaches its magnitude at the surface, and the daily amplitude begins to increase. At these depths, ΔT evolves approximately according to the dashed arrow.

the sample experiencing a larger amplitude temperature variation will have lower net retentivity over time. Similarly, because EDT is a function of activation energy, the EDT of cosmogenic ^{3}He in quartz will be different from that of cosmogenic ^{21}Ne in orthoclase within the same sample. The effects of temperature oscillations are magnified at lower temperatures; in other words, for the same amplitude temperature oscillation, ΔT increases with decreasing mean temperature.

ΔT does depend on frequency when multiple temperature oscillations occur simultaneously. To demonstrate this, Fig. 2 shows ΔT for periodic temperature functions with a mean of 0 °C and different daily and annual amplitudes for both the ^{3}He–quartz (A) and ^{21}Ne–feldspar (B) systems, calculated according to Eq. (4). Surfaces for mean temperatures other than 0 °C would plot sub-parallel to those shown in Fig. 2, with lower mean temperatures corresponding to greater ΔT values and divergence of the surfaces with increasing amplitudes.

In addition to heat conduction between rocks at the surface and surrounding air, rocks are also directly heated by incident solar radiation. The effects of radiative heating on rock temperature are complex and depend on factors such as the shortwave and longwave radiative fluxes, thermal properties of the rock like albedo, and short-term variables like moisture content, snow cover, and wind conditions (e.g. Deardorff, 1978; Hall et al., 2005; McGreevy, 1985). Barring stochastic, transient variables like wind, radiative heating has the same period as daily temperature oscillations and thus increases the magnitude of daily rock temperature amplitudes relative to that of air. Except in extreme desert environments, where the daily rock temperature amplitude can be as large as 40 °C (McFadden et al., 2005; McKay et al., 2003), 5–10 °C amplifications are typical, depending on albedo (Hall et al., 2005; McGreevy, 1985). Daily temperature amplitudes this large have significant effects on the ΔT, as shown in Fig. 2. Convolution of diurnal radiative heating of rock surfaces with daily and annual temperature oscillations can therefore result in large differences between EDT and mean temperature at the surface that need to be accounted for.

Since cosmogenic nuclide production occurs within a few meters of the Earth's surface and a typical sample moves with respect to the surface due to either erosion or aggradation, the attenuation of surface temperature variations with depth must also be considered. The amplitude of any surface temperature oscillation decreases with depth beneath the surface according to:

$$T(z) = A\exp\left(-z\sqrt{\frac{\omega\rho c_p}{2k}}\right)\exp\left(i\left[\omega t - z\sqrt{\frac{\omega\rho c_p}{2k}}\right]\right) \quad (5)$$

where T is temperature, z is depth, A is the surface temperature amplitude, ω is the surface temperature frequency, ρ is rock density, c_p is specific heat capacity, and k is thermal conductivity (e.g. Fowler, 2005). Fig. 3A shows solutions to Eq. (5) for the typical thermal properties and density of granite and for different frequency and amplitude surface temperature oscillations. Fig. 3A demonstrates that longer period temperature oscillations will propagate to greater depths. The skin depth—the depth at which the temperature amplitude decreases by $1/e$—is 0.14 m for daily and 2.8 m for annual oscillations; glacial cycle temperature oscillations affect temperatures tens to hundreds of meters beneath the surface. For comparison, the skin depth associated with the attenuation of cosmogenic nuclide production by spallation reactions in the same density material is 0.59 m (Fig. 3B). This indicates that cosmogenic nuclide production rates remain relatively high at depths where daily air and rock temperature oscillations are significantly diminished. The amplitude of the annual temperature oscillation, however, is significant at all depths where cosmogenic nuclide production occurs.

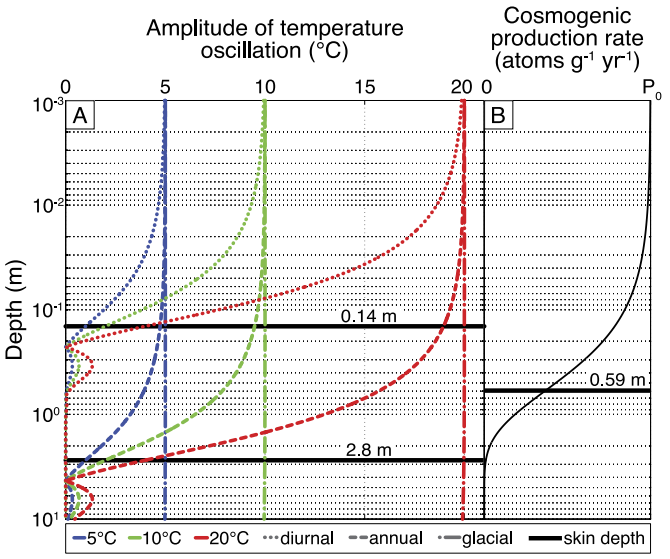

Fig. 3. Depth dependence of temperature perturbations originating at the surface (A) and cosmogenic nuclide production rates (B). In (A), we use the thermal properties of granite from McGreevy (1985) and a density of 2.7 g/cm^3 to calculate with Eq. (5) how thermal waves with diurnal, annual, and glacial-cycle periods with 5, 10, and 20 °C amplitudes at Earth's surface propagate with depth. The skin depth, the depth at which the amplitude of the temperature perturbation is $1/e$ of the surface amplitude, is noted for the different period oscillations. (B) Attenuation of a spallogenic cosmogenic nuclide production rate with depth, with a surface production rate of P_0. We assumed the same density as in (A) and an attenuation coefficient of 160 g/cm^2. The skin depth, the depth at which production equals P_0/e, is also shown. (For interpretation of the references to color in this figure, the reader is referred to the web version of this article.)

The arrows in Fig. 2A schematically demonstrate how daily and annual temperature oscillations influence the EDT and ΔT of a rock as it is brought to the surface by erosion for a constant mean surface temperature. At depths > ~0.14 m, the amplitudes of daily temperature oscillations (Fig. 3, dotted curves) are small and only the annual temperature oscillation (Fig. 3, dashed curves) will significantly affect ΔT. At these depths, ΔT (and EDT) evolves according to the solid arrow in Fig. 2A as the sample moves toward the surface and the amplitude of the annual temperature

oscillation increases. At depths $< \sim 0.14$ m, the amplitude of the daily temperature oscillation becomes significant, while the amplitude of the annual temperature oscillation approaches its surface magnitude; the ΔT will then evolve according to the dashed arrow in Fig. 2A. The reverse thermal history is expected for samples that are progressively buried due to sedimentation.

To summarize, rocks at Earth's surface are heated by surrounding air, which experiences temperature oscillations of predictable frequencies and amplitudes, and by solar radiation, which increases the amplitude of daily rock temperatures above that the surrounding air. Calculating a mean temperature from an observed diffusion temperature (i.e., EDT) of a cosmogenic noble gas–mineral system therefore requires considering the depth integrated effects of both diurnal radiative heating and short-term air temperature oscillations on rock temperatures. These short-term temperature oscillations should be predictable on long ($>10^3$ yr) timescales, as they are primarily a function of solar insolation and therefore latitude.

3. Methods

3.1. Assessing the sensitivity of cosmogenic noble gas paleothermometry

We present a series of calculations using the theory and mathematics outlined above to establish under what conditions cosmogenic noble gas–mineral pairs will record surface temperature histories. All calculations utilize the diffusion parameters for He in quartz reported by Shuster and Farley (2005) [$E_a = 84.5$ kJ/mol; $\ln(D_0/a^2) = 11.1$ $\ln(s^{-1})$]. We do not use the diffusion kinetics of ^{3}He in quartz reported by Trull et al. (1991), as their results were likely compromised by a nonuniform, unknown initial distribution of cosmogenic ^{3}He in their experiment. Gourbet et al. (2012) conducted diffusion experiments on multiple types of feldspars, demonstrating that feldspars generally experience diffusive loss of ^{21}Ne at Earth surface temperatures but that diffusion parameters are compositionally dependent. Since the diffusion experiment on MadOr orthoclase ($An_{0.2}Ab_{5.5}Or_{94.3}$) yielded the most robust, simple Arrhenius relationship for Ne diffusion (Gourbet et al., 2012), we use these parameters in our calculations [$E_a = 112.1$ kJ/mol; $\ln(D_0/a^2) = 7.4\ln(s^{-1})$]. For quartz, we use a sea level high-latitude (SLHL) cosmogenic production rate of 108 atoms/g/yr for ^{3}He (Vermeesch et al., 2009). Production rates of cosmogenic ^{21}Ne in feldspars vary depending on mineral composition. We use an SLHL production rate of 22.4 atoms/g/yr for the composition of MadOr orthoclase, calculated from the stoichiometric production rates of Gourbet et al. (2012) and the model production rates of Kober et al. (2005).

In the first set of calculations, we investigate the feasibility of estimating the integrated temperature over a single exposure period. We assume that production and the EDT are constant through time and use Eq. (3) to model the effects of grain size, temperature, and exposure duration on cosmogenic noble gas retention. Retention R, or the fraction of the cosmogenic noble gas produced that has not diffused from the mineral grain, can be defined as:

$$R = \left(\frac{M_A}{M_B}\right)\left(\frac{P_A}{P_B}\right)^{-1} \quad (6)$$

where A is a diffusive cosmogenic noble gas and B is a quantitatively-retained cosmogenic nuclide. Any cosmogenic nuclide that does not diffuse from the mineral or decay over the timescale of interest can be used as the quantitatively retained nuclide B; in the example dataset discussed later we use ^{10}Be. If both cosmogenic nuclides are quantitatively retained at the EDT, $R = 1$. If A is diffusively lost, R approaches zero over time as the concentration of A reaches steady-state and ingrowth of B continues. As defined in Eq. (6), R is readily calculated from laboratory measurements of A and B and knowledge of their production rate ratio.

In the second set of calculations, we evaluate the feasibility of estimating the magnitude of past temperature changes. We use the finite-difference scheme described by Ketcham (2005) to model how retention evolves for two geologic scenarios involving a temperature change. Production rates are scaled and passed to the forward model using the code underlying the CRONUS-Earth online calculator (Balco et al., 2008). In one scenario, we model cosmogenic noble gas retention for samples exposed since the last glacial period that experience rapid warming at the beginning of the Holocene. In another scenario, we model cosmogenic noble gas retention for samples exposed over the past 4 Ma that experience cooling across the Plio–Pleistocene climate transition. We allow the pre-transition EDTs to vary in each scenario and hold the post-transition EDT constant to evaluate whether the magnitude of a temperature shift can be resolved as differences in retention. We use both the modeled geologic scenarios and constant production and EDT calculations to discuss potential applications and limitations of cosmogenic noble gas paleothermometry for constraining past Earth surface temperatures.

3.2. Cosmogenic ^{3}He retention in Antarctic erratics

To evaluate whether the existing knowledge of diffusion kinetics for the ^{3}He–quartz system and the underlying theory are consistent with geologic observations, we measured cosmogenic ^{3}He abundances in quartz from glacially transported erratic cobbles in the Pensacola Mountains, Antarctica. While not originally collected for this purpose, these samples are useful for the present study because their cosmogenic ^{10}Be exposure ages define a monotonic exposure age–elevation relationship recording progressive deglaciation of this site between 10.6 and 4.8 ka. This relationship, which is commonly observed in similar data sets throughout Antarctica, indicates that each sample was emplaced during deglaciation and has experienced only a single period of surface exposure, and that the ^{10}Be exposure ages accurately record the duration of this period (e.g. Balco, 2011; Stone et al., 2003). Thus, given an exposure history determined from the ^{10}Be measurements and an estimate from present climatology of mean ambient temperatures in the Pensacola Mountains (ca. -25 to -30 °C; see discussion below), we compare measured ^{3}He concentrations with those predicted by Eq. (4) to evaluate whether using the open-system behavior of cosmogenic ^{3}He to reconstruct past temperatures is viable with natural samples.

4. Results and discussion

4.1. Effects of temperature, exposure duration, and grain size on cosmogenic noble gas retention

Figs. 4A–B show predicted retention, calculated with Eq. (3), of cosmogenic ^{3}He in quartz and ^{21}Ne in orthoclase as a function of time for constant-EDT exposure histories in 1 mm-diameter grains. These figures summarize the respective conclusions of the diffusion studies by Shuster and Farley (2005) and Gourbet et al. (2012): cosmogenic ^{3}He diffusion in quartz is significant at subzero EDTs and relatively short (10^3 yr) timescales, while cosmogenic ^{21}Ne diffusion in orthoclase is significant at EDTs in the 20–40 °C range on 10^5–10^6 yr timescales. Importantly, the calculations presented in Figs. 4A–B highlight the time and temperature ranges over which paleotemperature information could be constrained by cosmogenic noble gas observations. For example, EDTs ranging from -40 to 20 °C could readily be distinguished with measurements of cosmogenic ^{3}He retention in 1 mm quartz grains with

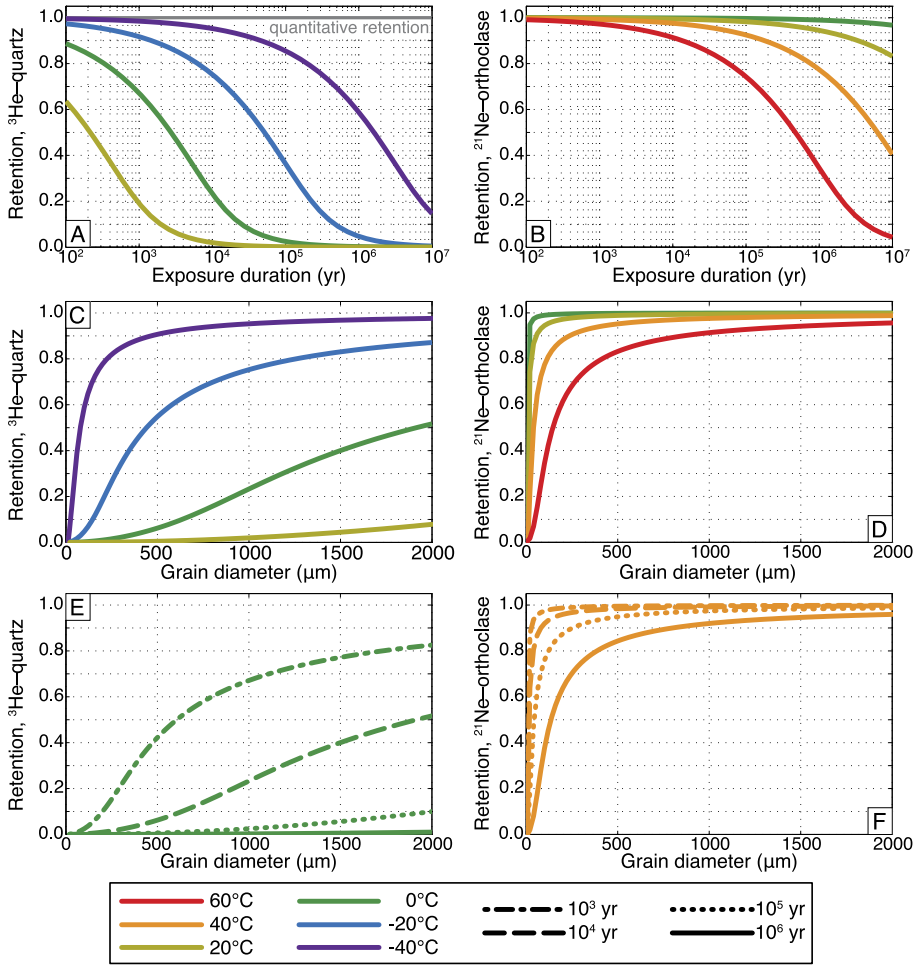

Fig. 4. Retention of cosmogenic ^{3}He in quartz (A, C, E) and ^{21}Ne in orthoclase feldspar (B, D, F) using the diffusion kinetics of Shuster and Farley (2005) and Gourbet et al. (2012), respectively. Retention refers to the fraction of the cosmogenic noble gas produced during exposure that has not diffused from the mineral grain. Curves were calculated using the analytical solution of the production–diffusion equation (Eq. (3)) assuming a constant effective diffusion temperature (EDT). In (A) and (B), retention is plotted as a function of EDT and exposure duration for 1 mm-diameter grains, assuming that the grain size defines the size of the diffusion domain. The line for quantitative retention (i.e. no diffusion during exposure) is also shown in (A). (C) and (D) show retention as a function of EDT and grain size for an exposure duration of 10^4 yr. In (E) and (F), retention is shown as a function of grain size and exposure duration. In (E), retention curves are plotted for an EDT of 0 °C; in (F), the EDT = 40 °C. (For interpretation of the references to color in this figure, the reader is referred to the web version of this article.)

10 ka exposure durations. However, for the same grain size and exposure duration, cosmogenic ^{21}Ne is quantitatively retained in orthoclase ($R = 1$) at all EDTs below 40 °C; this nuclide–mineral pair would only display partial retention at typical Earth surface temperatures for exposure durations $>10^6$ yr. The results of Gourbet et al. (2012) imply that cosmogenic ^{21}Ne retention in other alkali feldspars (anorthoclase and sanidine) should be sensitive to a lower temperature range over shorter exposure durations than ^{21}Ne in orthoclase. Available data predict complete retention of cosmogenic ^{21}Ne in quartz at all EDTs and timescales shown in Fig. 4, indicating that this nuclide–mineral pair is expected to always accurately record exposure duration.

Broadly, these results indicate that the ratio of cosmogenic ^{3}He to a quantitatively retained cosmogenic nuclide in quartz can constrain past surface temperatures in polar and high altitude environments, where EDTs are consistently at or below 0 °C. The concentration of the fully-retained nuclide (e.g., ^{21}Ne, ^{10}Be, or ^{26}Al) constrains the exposure duration, while the concentration of cosmogenic ^{3}He can be used to determine the EDT. ^{21}Ne measurements in orthoclase can constrain paleotemperature histories at lower latitudes and elevations than the ^{3}He–quartz system, where EDTs are in the 20–40 °C range.

Retention, and hence the useful temperature range of a particular nuclide–mineral pair, depends on grain size; Figs. 4C–F show this effect. Larger grains, corresponding to larger diffusion domains, display higher retentivity at a given EDT and duration for both systems. This is potentially advantageous for paleothermometry because of the possibility of selecting grain sizes to yield maximum sensitivity for particular geologic problems and temperature ranges. For example, while cosmogenic ^{21}Ne is expected to be fully retained in orthoclase at EDTs $\leq$40 °C in 1 mm-diameter grains for 10^4 yr of exposure (Fig. 4B), significant temperature-retention differences are predicted for the same scenario in 0.1 mm-diameter grains (Fig. 4D). Additionally, observations of retention in different grain sizes can provide an important test for internal consistency: observed retentivities in different grain sizes with a common exposure history should imply a common EDT.

4.2. Geologic scenarios involving temperature change

While constant EDT-exposure scenarios are useful for demonstrating the temperature sensitivity of various nuclide–mineral pairs, geologic applications of open-system behavior of cosmogenic noble gases will most likely be aimed at reconstructing past temperature changes. To explore this, we consider two hypothetical geologic scenarios in which the timing of a temperature change is well established but its magnitude in a particular location is not.

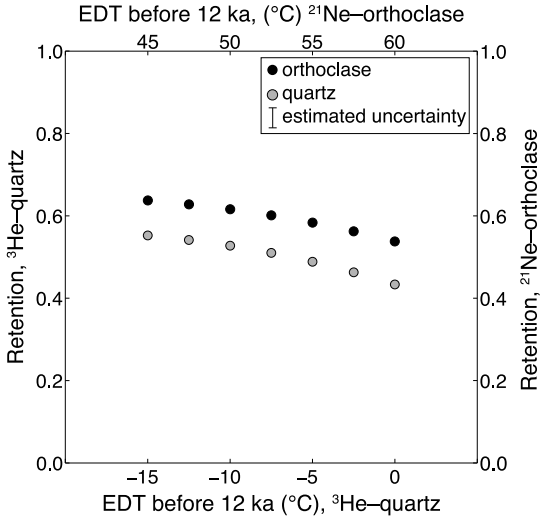

Fig. 5. Example geologic scenario where cosmogenic noble gas retention is modeled for different magnitude temperature changes at the transition between the last glacial period and the Holocene Epoch. All calculations assume exposure began at 16 ka and warming occurred over a 1.2 ka period centered at 12 ka. Retention of cosmogenic ^{3}He in quartz (left, gray circles) is plotted against effective diffusion temperature (EDT) before the increase centered at 12 ka (bottom). The predicted ^{3}He retention corresponds to 2 mm-diameter quartz grains that have experienced an EDT of 0 °C over the Holocene. Retention of cosmogenic ^{21}Ne in orthoclase feldspar (right, black circles) is plotted against EDT before the increase centered at 12 ka (top). The predicted ^{21}Ne retention corresponds to 0.2 mm-diameter orthoclase grains that have experienced an EDT of 60 °C over the Holocene. We assume an average erosion rate of 5 m/Ma for both systems, although the results are relatively insensitive to erosion rate on this timescale.

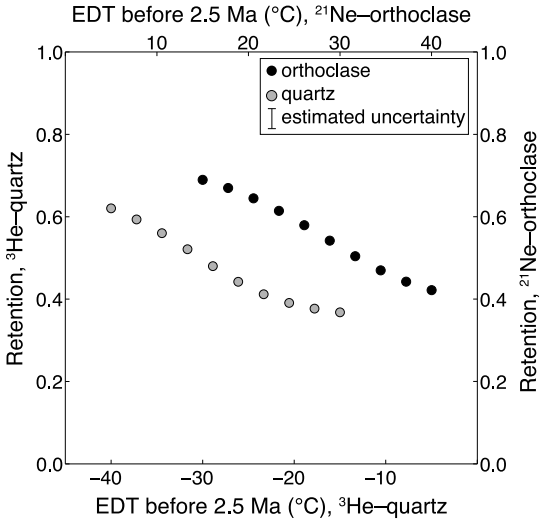

Fig. 6. Example geologic scenario where cosmogenic noble gas retention is modeled for different magnitude temperature changes at the Pliocene–Pleistocene transition. All calculations assume exposure began at 4 Ma and cooling occurred over a 0.25 Ma period centered at 2.5 Ma. Retention of cosmogenic ^{3}He in quartz (left, gray circles) is plotted against effective diffusion temperature (EDT) before the decrease centered at 2.5 Ma (bottom). The predicted ^{3}He retention corresponds to 2 mm-diameter quartz grains that have experienced an EDT of −40 °C over the Quaternary Period. Retention of cosmogenic ^{21}Ne in orthoclase feldspar (right, black circles) is plotted against EDT before the decrease centered at 2.5 Ma (top). The predicted ^{21}Ne retention corresponds to 0.2 mm-diameter orthoclase grains that have experienced an EDT of 15 °C over the Quaternary. An average erosion rate of 0.1 m/Myr is assumed for both systems.

A variety of paleoenvironmental and geochemical proxies from marine or lacustrine sediments and ice cores have been used to estimate the magnitude of local and globally-averaged warming at the end of the last glacial period (e.g. Clark et al., 2012; Shakun et al., 2012). In continental settings, these proxies often only provide qualitative estimates of temperature change (Bartlein et al., 2011; Farrera et al., 1999). Quantitative estimates of continental temperatures for the last glacial maximum have been made from plant macrofossils and pollen records; however, in many cases these estimates cannot be reconciled with sea surface temperature proxies and climate models to better than 4–8 °C (Annan and Hargreaves, 2013) despite nominally having an uncertainty of only 1–2 °C (Farrera et al., 1999, and references therein).

In Fig. 5, we show model calculations that evaluate whether cosmogenic noble gas paleothermometry could be used to determine the magnitude of continental temperature increases at the onset of the Holocene. We assume that a sample has been continuously exposed for 16 ka at an erosion rate of 5 m/Ma. A single warming event occurs over a 1.2 ka period centered at 12 ka. We consider two cases that are suited to the ^{3}He–quartz and ^{21}Ne–orthoclase pairs, respectively: Holocene EDTs of 0 °C are typical of high elevations in low to mid-latitude mountainous regions, while EDTs of 60 °C occur in arid deserts where radiative solar heating is significant.

Fig. 5 demonstrates that retention of ^{3}He in quartz and ^{21}Ne in orthoclase is sensitive to the magnitude of Holocene warming in both scenarios. However, for scenarios such as this one in which temperatures increase through time, the sensitivity is relatively small, as the increase in diffusivity caused by climate warming acts to speed up the loss of information about the prior colder period. Retention varies by <20% between scenarios in which EDTs during the last glacial period equaled the Holocene EDT and were 15 °C cooler. Assuming that measurements of retention can be resolved with ±2.5% precision, one could determine pre-Holocene EDTs (and infer mean Holocene temperatures) to within ±2.5 °C. In some cases, this would improve upon existing estimates, or provide quantitative constraints where only qualitative estimates presently exist. Measurements of retention across multiple grain sizes could in principle provide greater temperature resolution in this scenario.

Our second scenario involves the Pliocene–Pleistocene climate transition, which is marked by cooling and the onset of northern hemisphere continental glaciation at ∼2.5 Ma (Balco and Rovey, 2010; Haug et al., 2005; Raymo, 1994). Paleotemperature estimates for the Pliocene are scarce and frequently qualitative, particularly on continental settings and at low latitudes. Cosmogenic noble gas concentrations in rocks in very slowly eroding landscapes that have resided at or near the surface since before ∼2.5 Ma should record the magnitude of cooling across this transition. Rock surfaces with apparent exposure ages exceeding 2.5 Ma are common in the polar deserts of the Transantarctic Mountains (Schäfer et al., 1999) and the low-latitude deserts of Australia (Fujioka et al., 2005), Chile (Dunai et al., 2005; Evenstar et al., 2009), and Namibia (Bierman and Caffee, 2001), and likely exist in other arid and tectonically quiescent regions.

Fig. 6 shows predicted retention of cosmogenic ^{3}He in quartz and ^{21}Ne in orthoclase for an exposure scenario in which samples are continuously exposed for 4 Ma at a constant erosion rate of 0.1 m/Ma. A single cooling event occurs over a 0.25 Ma period centered at 2.5 Ma. We assume the same grain sizes as in the previous example, but EDTs of −40 °C for quartz (typical of the Transantarctic Mountains) and 15 °C for orthoclase (typical of moderate elevations at temperate latitudes) during the Quaternary. In contrast to the previous example, a scenario in which temperature and therefore diffusivity decreases over time tends to increase the preservation of past temperature information. The same conceptual model could be applied to samples exposed at the surface during the Pliocene and subsequently buried in a sedimentary deposit at depths where cosmogenic production is negligible.

4.3. An initial test of cosmogenic noble gas paleothermometry with geologic samples

While diffusion experiments enable predictions of retentivity for a particular cosmogenic noble gas–mineral pair as in Sections 4.1 and 4.2, these predictions have yet to be tested directly with geologic samples. To do this, we measured cosmogenic ^{3}He and ^{10}Be in nine quartz samples from an elevation transect of glacially transported cobbles in the Pensacola Mountains, Antarctica (Table 1; see Tables S1–S3 for additional sample, site, and analytical information). As previously mentioned, all samples have ^{10}Be exposure ages younger than 11 ka that define a monotonic age–elevation relationship, suggesting a single period of surface exposure for each sample as deglaciation progressed during the Holocene (e.g. Stone et al., 2003).

Our goal in presenting these data is not to reconstruct a detailed Holocene temperature history for Antarctica. Rather, we use these data to examine whether the temperatures inferred from cosmogenic noble gases agree with the relatively simple climatological and surface exposure histories that we expect for these samples. Thus we make several simplifying assumptions in our analysis and interpretation of this dataset. First, we assume that the ^{3}He diffusion kinetics determined by Shuster and Farley (2005) apply to the quartz samples we analyzed and do not take into account uncertainty in the diffusion kinetics. Second, we do not incorporate production rate uncertainties of either ^{3}He or ^{10}Be into our analysis. And lastly, although we analyzed quartz grains between 0.25 and 0.85 mm in diameter (representative of the range of quartz grain sizes in the samples, which are medium to coarse grained sandstones), we assume a representative grain size of 0.5 mm in our calculations. We then use apparent ^{3}He and ^{10}Be exposure ages and these assumptions to calculate an average EDT for all samples and compare this EDT to that expected from the climatology of the sample location. For future quantitative paleotemperature reconstructions, sample-specific diffusion kinetics and more rigorous quantification of grain size and the ^{3}He/^{10}Be production rate ratio will be necessary, since each of our assumptions affects the calculation of an EDT and potentially introduces non-trivial uncertainty into our analysis.

Apparent ^{3}He exposure ages are systematically younger than ^{10}Be exposure ages of these samples (Fig. 7A), consistent with diffusive loss of ^{3}He at surface exposure temperatures and resulting in ^{3}He retention of ~28–63% (Fig. 7B). In calculating apparent ^{3}He exposure ages, we assume that the ^{3}He observed in our samples is cosmogenic ^{3}He produced solely during the most recent period of exposure, which is consistent with the simple exposure history inferred from the ^{10}Be exposure ages. Given the diffusion kinetics of ^{3}He in quartz (Shuster and Farley, 2005), any non-cosmogenic ^{3}He present at the time of mineral formation (e.g. from magmatic gases or hydrothermal fluids) is expected to be rapidly lost by diffusion. We applied the finite difference scheme used in Section 4.2 to iteratively calculate the EDT that best predicts the observed ^{3}He retention for each sample; the average EDT for all samples, accounting for measurement uncertainty only, is -13 ± 4 °C (Fig. 7C).

The curves in Figs. 7A–B show the expected relationship between apparent ^{3}He exposure age and ^{3}He retention with exposure duration for several constant EDTs. Although there is an apparent structure in the ^{3}He retention–exposure age relationship that varies from the expected relationship for a constant EDT of −13 °C, the reduced chi-squared misfit between the observed ^{3}He retention and that predicted for an EDT of −13 °C is 1.04, suggesting that most of this variability can be explained by uncertainty in the ^{3}He measurements. Additional variability may also result from differences in sample-specific diffusion kinetics (Tremblay et al., 2013), the grain size distribution of ^{3}He analysis aliquots, site-specific differences in radiative heating, or some

Table 1
Cosmogenic ^{10}Be and ^{3}He concentrations in quartz, apparent surface exposure ages, and implied ^{3}He retention for glacially transported cobbles from the Pensacola, Antarctica. Analytical details appear in supplementary Tables S1–S3. To calculate exposure ages, we used version 2.2 of the CRONUS-Earth online calculator (Balco et al., 2008) with the scaling scheme of Stone (2000), the production rate calibration dataset of Balco et al. (2009) for ^{10}Be, and the production rate estimate of Vermeesch et al. (2009) for ^{3}He. We also assume a rock density of 2.5 g/cm^{3}, an attenuation coefficient of 160 g/cm^{2}.

Sample name	Latitude (DD)	Longitude (DD)	Elevation (m)	[^{10}Be] (10^{3} atoms/g)[a]	[^{3}He] (10^{3} atoms/g)	Apparent exposure ages (yr)		^{3}He retention
						[^{10}Be][b]	[^{3}He][b]	
10-MPS-077-CRK	−83.6368	−59.0117	488	39.2 ± 1.2	569 ± 106	4837 ± 144	2622 ± 664	0.54 ± 0.14
10-MPS-095-CRK	−83.6420	−58.9552	576	50.5 ± 2.5	502 ± 116	5757 ± 281	2139 ± 1197	0.37 ± 0.21
10-MPS-099-CRK	−83.6394	−58.9785	565	56.1 ± 1.5	541 ± 282	6512 ± 176	2349 ± 763	0.36 ± 0.12
10-MPS-120-IBR	−83.8094	−58.8613	632	37.3 ± 1.2	627 ± 115	4114 ± 132	2584 ± 544	0.63 ± 0.13
10-MPS-123-HBS	−83.7455	−58.8309	996	132.4 ± 2.8	1551 ± 132	10612 ± 226	4614 ± 672	0.435 ± 0.064
10-MPS-124-LNK	−83.7596	−59.0759	812	87.3 ± 2.2	886 ± 134	8287 ± 210	3134 ± 743	0.378 ± 0.090
10-MPS-126-LNK	−83.7608	−59.0739	806	87.1 ± 2.2	892 ± 106	8592 ± 213	3278 ± 783	0.382 ± 0.092
10-MPS-128-LNK	−83.7589	−59.0778	755	69.2 ± 2.0	520 ± 130	6853 ± 198	1920 ± 731	0.28 ± 0.11
10-MPS-129-LNK	−83.7589	−59.0778	755	67.7 ± 1.7	575 ± 94	6859 ± 169	2169 ± 638	0.316 ± 0.093

[a] Concentrations normalized to '07KNSTD' standardization (Nishiizumi et al., 2007). See supplementary data.
[b] Uncertainties are 'internal' uncertainties including measurement uncertainty only.

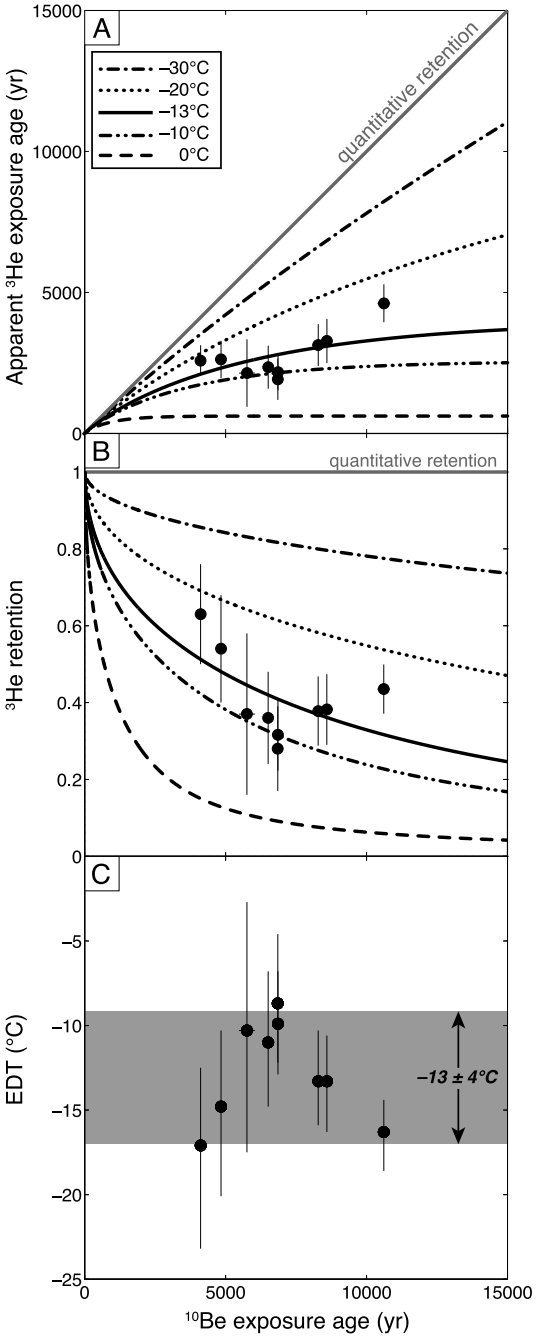

Fig. 7. Retention of cosmogenic ^{3}He in glacial erratics with simple Holocene exposure histories from the Pensacola Mountains, Antarctica. ^{10}Be concentrations in quartz constrain the exposure duration of each sample, and we estimated apparent exposure ages from measurements of ^{3}He in quartz from the same samples and assuming all ^{3}He was cosmogenic. (A) shows the relationship between the apparent ^{3}He exposure age and the ^{10}Be exposure age; if no ^{3}He diffusion occurred, all data points would plot on the line labeled 'quantitative retention'. (B) shows the relationship between retention of cosmogenic ^{3}He (apparent ^{3}He exposure age/^{10}Be exposure age) and ^{10}Be exposure age. Uncertainties shown in (A) and (B) include measurement uncertainties only. Uncertainties in ^{10}Be exposure ages are in most cases smaller than the symbol plotted. Curves in (A) and (B) show how apparent ^{3}He exposure age and retention evolve with time for different effective diffusion temperatures (EDTs), respectively. In (C), we calculated the EDT from the ^{3}He retention and exposure duration (from the ^{10}Be measurements) of each sample. If we assume that the EDT for all samples is equal and has been invariant over their respective exposure histories, we find an average EDT in the Pensacola Mountains during the Holocene of $-13 \pm 4\,^{\circ}$C. This corresponds to a mean annual temperature between -25 and $-30\,^{\circ}$C (see text).

combination therein. Because retention in each sample integrates over its thermal history, it is very unlikely that the apparent structure in the ^{3}He dataset results from several degree temperature changes over short time intervals (i.e. several hundred years) during the Holocene. This variability is also unlikely caused by a local lapse rate, as katabatic winds prevent typical lapse rates in places like the Pensacola Mountains (Nylen et al., 2004).

Numerous ice core paleotemperature reconstructions for Antarctica show that Holocene temperature changes in inland regions were small (e.g. Jouzel et al., 2001; Masson et al., 2000). Given that mean temperatures in the Pensacola Mountains remained relatively constant over the Holocene, we can compare this average EDT of $\sim -13\,^{\circ}$C to mean temperature using the reasoning outlined in Section 2.3. The automated weather stations (AWS) from the University of Wisconsin–Madison AWS Program nearest the Pensacola Mountains in latitude and elevation are Elizabeth (82.6°S, 137.1°W; 549 m), Erin (84.9°S, 128.8°W; 990 m), and Harry (83.0°S, 121.4°W; 954 m). In addition to daily and annual oscillations, temperatures at these sites vary sub-annually, and the amplitude of daily oscillations decreases dramatically from the austral summer to winter. These short-term oscillations and the average mean annual temperature (MAT) at these AWS sites of $-23 \pm 2\,^{\circ}$C are likely very similar to those occurring in the Pensacola Mountains. The average EDT for the three AWS sites, calculated from three-hour temperature data collected from 2009 to 2012, is $-16 \pm 1\,^{\circ}$C. This EDT is consistent with the Holocene EDT estimated from our ^{3}He retention measurements. Because we have not accounted for the effects of radiative heating on rock temperatures during the austral summer, the difference between MAT and EDT in the Pensacola Mountains may be even greater, suggesting colder MATs in the Pensacola Mountains. This is consistent with MAT estimates from 10m firn temperatures on the Ronne Ice Shelf (adjacent to the Pensacola Mountains) of $-30\,^{\circ}$C (Graf et al., 1999). Overall, an estimated modern MAT in the Pensacola Mountains between -25 and $-30\,^{\circ}$C is consistent with the Holocene EDT calculated from cosmogenic ^{3}He measurements in quartz. This result demonstrates that, when combined with the theory and principles applied to radiogenic noble gases, our current knowledge about the production and diffusion of cosmogenic ^{3}He in quartz are consistent with observations of cosmogenic ^{3}He in geologic samples exposed at surface temperatures.

5. Conclusions

The open-system behavior of cosmogenic noble gases in common minerals like quartz and feldspars can be interpreted using the theory and mathematics applied to radiogenic noble gas thermochronometers and used to reconstruct past Earth surface temperatures. Calculations based on published diffusion kinetics predict that the cosmogenic ^{3}He–quartz system is sensitive to subzero temperatures characteristic of high elevation and/or high altitude environments, while the ^{21}Ne–orthoclase system is sensitive to moderate to high temperatures on geologic timescales. Both systems can potentially resolve temperature changes associated with climatic events during the past few million years. Applications of cosmogenic noble gas thermochronometry will require careful consideration of the fundamentally noisy thermal histories rocks experience near Earth's surface, but we demonstrate that short-term temperature fluctuations can be accounted for with effective diffusion temperatures. This new technique should be valuable for corroborating existing paleotemperature proxy records where they exist and expanding their spatial and temporal resolution where they do not.

Acknowledgements

We thank C. Todd for collecting some of the samples from the Pensacola Mountains as well as M. Vermeulen and M. Hegland for assistance with sample collection and preparation. We appreciate AWS three-hour temperature datasets made available by the University of Wisconsin–Madison AWS Program, supported by the NSF Antarctic Sciences Program (ANT-0944018 and ANT-1245663; http://amrc.ssec.wisc.edu). B. Guralnik and an anonymous referee provided detailed reviews that helped clarify this manuscript. We acknowledge support from the NSF Petrology and Geochemistry Program (EAR-1322086), the UC Berkeley Larsen Grant, and the Ann and Gordon Getty Foundation.

Appendix A. Supplementary material

Supplementary material related to this article can be found online at http://dx.doi.org/10.1016/j.epsl.2014.05.040.

References

Ackert Jr., R.P., Mukhopadhyay, S., Pollard, D., DeConto, R.M., Putnam, A.E., Borns Jr., H.W., 2011. West Antarctic Ice Sheet elevations in the Ohio Range: geologic constraints and ice sheet modeling prior to the last highstand. Earth Planet. Sci. Lett. 307, 83–93.

Annan, J.D., Hargreaves, J.C., 2013. A new global reconstruction of temperature changes at the Last Glacial Maximum. Clim. Past 9, 367–376.

Balco, G., 2011. Contributions and unrealized potential contributions of cosmogenic-nuclide exposure dating to glacier chronology, 1990–2010. Quat. Sci. Rev. 30, 3–27.

Balco, G., Briner, J., Finkel, R.C., Rayburn, J.A., Ridge, J.C., Schaefer, J.M., 2009. Regional beryllium-10 production rate calibration for late-glacial northeastern North America. Quat. Geochronol. 4, 93–107.

Balco, G., Rovey, C.W., 2010. Absolute chronology for major Pleistocene advances of the Laurentide Ice Sheet. Geology 38, 795–798.

Balco, G., Stone, J.O., Lifton, N.A., Dunai, T.J., 2008. A complete and easily accessible means of calculating surface exposure ages or erosion rates from ^{10}Be and ^{26}Al measurements. Quat. Geochronol. 3, 174–195.

Bartlein, P.J., Harrison, S.P., Brewer, S., Connor, S., Davis, B.A.S., Gajewski, K., Guiot, J., Harrison-Prentice, T.I., Henderson, A., Peyron, O., Prentice, I.C., Scholze, M., Seppä, H., Shuman, B., Sugita, S., Thompson, R.S., Viau, A.E., Williams, J., Wu, H., 2011. Pollen-based continental climate reconstructions at 6 and 21 ka: a global synthesis. Clim. Dyn. 37, 775–802.

Baxter, E.F., 2010. Diffusion of noble gases in minerals. Rev. Mineral. Geochem. 72, 509–557.

Bierman, P.R., Caffee, M., 2001. Slow rates of rock surface erosion and sediment production across the Namib Desert and Escarpment, southern Africa. Am. J. Sci. 301, 326–358.

Brook, E.J., Kurz, M.D., 1993. Surface-exposure chronology using in situ cosmogenic ^{3}He in antarctic quartz sandstone boulders. Quat. Res. 39, 1–10.

Brook, E.J., Kurz, M.D., Ackert Jr., R.P., Denton, G.H., Brown, E.T., Raisbeck, G.M., Yiou, F., 1993. Chronology of glacier advances in Arena Valley, Antarctica, using in situ cosmogenic ^{3}He and ^{10}Be. Quat. Res. 39, 11–23.

Brook, E.J., Kurz, M.D., Ackert, R.P., Raisbeck, G., Yiou, F., 1995. Cosmogenic nuclide exposure ages and glacial history of late Quaternary Ross Sea drift in McMurdo Sound, Antarctica. Earth Planet. Sci. Lett. 131, 41–56.

Bruno, L.A., Baur, H., Graf, T., Schluchter, C., Signer, P., Wieler, R., 1997. Dating of Sirius Group tillites in the Antarctic Dry Valleys with cosmogenic ^{3}He and ^{21}Ne. Earth Planet. Sci. Lett. 147, 37–54.

Cerling, T.E., 1990. Dating geomorphologic surfaces using cosmogenic ^{3}He. Quat. Res. 33, 148–156.

Cherniak, D.J., Thomas, J.B., Watson, E.B., 2014. Neon diffusion in olivine and quartz. Chem. Geol. 371, 68–82.

Christodoulides, C., Ettinger, K.V., Fremlin, J.H., 1971. The use of TL glow peaks at equilibrium in the examination of the thermal and radiation history of materials. Mod. Geol. 2, 275–280.

Clark, P.U., Shakun, J.D., Baker, P.A., Bartlein, P.J., Brewer, S., Brook, E., Carlson, A.E., Cheng, H., Kaufman, D.S., Liu, Z., Marchitto, T.M., Mix, A.C., Morrill, C., Otto-bliesner, B.L., Pahnke, K., Russell, J.M., Whitlock, C., Adkins, J.F., Blois, J.L., Clark, J., Colman, S.M., Curry, W.B., Flower, B.P., He, F., Johnson, T.C., Lynch-Stieglitz, J., Markgraf, V., McManus, J., Mitrovica, J.X., Moreno, P.I., Williams, J.W., 2012. Global climate evolution during the last deglaciation. Proc. Natl. Acad. Sci. USA 109.

Craig, H., Poreda, R.J., 1986. Cosmogenic He in terrestrial rocks: the summit lavas of Maui. Proc. Natl. Acad. Sci. USA 83, 1970–1974.

Deardorff, J.W., 1978. Efficient prediction of ground surface temperature and moisture, with inclusion of a layer of vegetation. J. Geophys. Res. 83, 1889.

Dohmen, R., Milke, R., 2010. Diffusion in polycrystalline materials: grain boundaries, mathematical methods, and experimental data. Rev. Mineral. Geochem. 72, 921–970.

Dunai, T.J., 2010. Cosmogenic Nuclides: Principles, Concepts, and Applications in the Earth Surface Sciences. Cambridge University Press, New York.

Dunai, T.J., González López, G.A., Juez-Larré, J., 2005. Oligocene–Miocene age of aridity in the Atacama Desert revealed by exposure dating of erosion-sensitive landforms. Geology 33, 321.

Durrani, S.A., Prachyabrued, W., Christodoulides, C., Fremlin, J.H., 1972. Thermoluminescence of Apollo 12 samples: implications for lunar temperature and radiation histories. In: Lunar and Planetary Science Conference Proceedings, pp. 2955–2970.

Eiler, J.M., 2007. "Clumped-isotope" geochemistry—The study of naturally-occurring, multiply-substituted isotopologues. Earth Planet. Sci. Lett. 262, 309–327.

Eiler, J.M., 2011. Paleoclimate reconstruction using carbonate clumped isotope thermometry. Quat. Sci. Rev. 30, 3575–3588.

Evenstar, L.A., Hartley, A.J., Stuart, F.M., Mather, A.E., Rice, C.M., Chong, G., 2009. Multiphase development of the Atacama Planation Surface recorded by cosmogenic ^{3}He exposure ages: implications for uplift and Cenozoic climate change in western South America. Geology 37, 27–30.

Farley, K.A., Shuster, D.L., Watson, E.B., Wanser, K.H., Balco, G., 2010. Numerical investigations of apatite ^{4}He/^{3}He thermochronometry. Geochem. Geophys. Geosyst. 11.

Farrera, I., Harrison, S.P., Prentice, I.C., Ramstein, G., Guiot, J., Bartlein, P.J., Bonnefille, R., Bush, M., Cramer, W., von Grafenstein, U., Holmgren, K., Hooghiemestra, H., Hope, G., Jolly, D., Lauritzen, S.-E., Ono, Y., Pinot, S., Stute, M., Yu, G., 1999. Tropical climates at the Last Glacial Maximum: a new synthesis of terrestrial palaeoclimate data. I. Vegetation, lake-levels and geochemistry. Clim. Dyn. 15, 823–856.

Forest, C.E., Wolfe, J.A., Molnar, P., Emanuel, K.A., 1999. Paleoaltimetry incorporating atmospheric physics and botanical estimates of paleoclimate. Geol. Soc. Am. Bull. 111, 497–511.

Fowler, C.M.R., 2005. The Solid Earth: An Introduction to Global Geophysics, 2nd ed. Cambridge University Press, Cambridge, UK.

Fujioka, T., Chappell, J., Honda, M., Yatsevich, I., Fifield, K., Fabel, D., 2005. Global cooling initiated stony deserts in central Australia 2–4 Ma, dated by cosmogenic ^{21}Ne–^{10}Be. Geology 33, 993.

Ghosh, P., Adkins, J., Affek, H., Balta, B., Guo, W., Schauble, E.A., Schrag, D., Eiler, J.M., 2006. ^{13}C–^{18}O bonds in carbonate minerals: a new kind of paleothermometer. Geochim. Cosmochim. Acta 70, 1439–1456.

Gosse, J.C., Phillips, F.M., 2001. Terrestrial in situ cosmogenic nuclides: theory and application. Quat. Sci. Rev. 20, 1475–1560.

Gourbet, L., Shuster, D.L., Balco, G., Cassata, W.S., Renne, P.R., Rood, D., 2012. Neon diffusion kinetics in olivine, pyroxene and feldspar: retentivity of cosmogenic and nucleogenic neon. Geochim. Cosmochim. Acta 86, 21–36.

Graf, W., Reinwarth, O., Oerter, H., Mayer, C., Lambrecht, A., 1999. Surface accumulation on Foundation Ice Stream, Antarctica. Ann. Glaciol. 29, 23–28.

Granger, D.E., Lifton, N.A., Willenbring, J.K., 2013. A cosmic trip: 25 years of cosmogenic nuclides in geology. Geol. Soc. Am. Bull. 125, 1379–1402.

Gregory, K.M., McIntosh, W.C., 1996. Paleoclimate and paleoelevation of the Oligocene Pitch-Pinnacle flora, Sawatch Range, Colorado. Geol. Soc. Am. Bull. 108, 545–561.

Hall, K., Lindgren, B.S., Jackson, P., 2005. Rock albedo and monitoring of thermal conditions in respect of weathering: some expected and some unexpected results. Earth Surf. Process. Landf. 30, 801–811.

Harrison, T.M., Zeitler, P.K., 2005. Fundamentals of noble gas thermochronometry. Rev. Mineral. Geochem. 58, 123–149.

Haug, G.H., Ganopolski, A., Sigman, D.M., Rosell-Mele, A., Swann, G.E.A., Tiedemann, R., Jaccard, S.L., Bollmann, J., Maslin, M.A., Leng, M.J., Eglinton, G., 2005. North Pacific seasonality and the glaciation of North America 2.7 million years ago. Nature 433, 821–825.

Ivy-Ochs, S., Kober, F., Alfimov, V., Kubik, P.W., Synal, H.-A., 2007. Cosmogenic ^{10}Be, ^{21}Ne and ^{36}Cl in sanidine and quartz from Chilean ignimbrites. Nucl. Instrum. Methods Phys. Res., Sect. B, Beam Interact. Mater. Atoms 259, 588–594.

Jouzel, J., Masson, V., Cattani, O., Falourd, S., Stievenard, M., Stenni, B., Longinelli, A., Johnsen, S.J., Steffenssen, J.P., Petit, J.R., Schwander, J., Souchez, R., Barkov, N.I., 2001. A new 27 ky high resolution East Antarctic climate record. Geophys. Res. Lett. 28, 3199–3202.

Jungers, M.C., Heimsath, A.M., Amundson, R., Balco, G., Shuster, D., Chong, G., 2013. Active erosion–deposition cycles in the hyperarid Atacama Desert of Northern Chile. Earth Planet. Sci. Lett. 371–372, 125–133.

Ketcham, R.A., 2005. Forward and inverse modeling of low-temperature thermochronometry data. Rev. Mineral. Geochem. 58 (1), 275–314.

Kim, S.-T., O'Neil, J.R., 1997. Equilibrium and nonequilibrium oxygen isotope effects in synthetic carbonates. Geochim. Cosmochim. Acta 61, 3461–3475.

Kober, F., Ivy-Ochs, S., Leya, I., Baur, H., Magna, T., Wieler, R., Kubik, P.W., 2005. In situ cosmogenic ^{10}Be and ^{21}Ne in sanidine and in situ cosmogenic ^{3}He in Fe–Ti-oxide minerals. Earth Planet. Sci. Lett. 236, 404–418.

Kober, F., Ivy-Ochs, S., Schlunegger, F., Baur, H., Kubik, P.W., Wieler, R., 2007. Denudation rates and a topography-driven rainfall threshold in northern Chile: multiple cosmogenic nuclide data and sediment yield budgets. Geomorphology 83, 97–120.
Kurz, M.D., 1986. Cosmogenic helium in a terrestrial igneous rock. Nature 320, 435–439.
Lal, D., 1991. Cosmic ray labeling of erosion surfaces: in situ nuclide production rates and erosion models. Earth Planet. Sci. Lett. 104, 424–439.
Marti, K., Craig, H., 1987. Cosmic-ray-produced neon and helium in the summit lavas of Maui. Nature 325, 335–337.
Masson, V., Vimeux, F., Jouzel, J., Morgan, V., Delmotte, M., Ciais, P., Hammer, C., Johnsen, S., Lipenkov, V.Y., Mosley-Thompson, E., Petit, J.-R., Steig, E.J., Stievenard, M., Vaikmae, R., 2000. Holocene climate variability in Antarctica based on 11 ice-core isotopic records. Quat. Res. 54, 348–358.
McFadden, L.D., Eppes, M.C., Gillespie, A.R., Hallet, B., 2005. Physical weathering in arid landscapes due to diurnal variation in the direction of solar heating. Geol. Soc. Am. Bull. 117, 161.
McGreevy, J.P., 1985. Thermal properties as controls on rock surface temperature maxima, and possible implications for rock weathering. Earth Surf. Process. Landf. 10, 125–136.
McKay, C.P., Friedmann, E.I., Gómez-Silva, B., Cáceres-Villanueva, L., Andersen, D.T., Landheim, R., 2003. Temperature and moisture conditions for life in the extreme arid region of the Atacama desert: four years of observations including the El Nino of 1997–1998. Astrobiology 3, 393–406.
Meesters, A.G.C.A., Dunai, T.J., 2002. Solving the production–diffusion equation for finite diffusion domains of various shapes. Part I. Implications for low-temperature (U–Th)/He thermochronology. Chem. Geol. 186, 333–344.
Nishiizumi, K., Imamura, M., Caffee, M.W., Southon, J.R., Finkel, R.C., McAninch, J., 2007. Absolute calibration of ^{10}Be AMS standards. Nucl. Instrum. Methods Phys. Res. B 258, 403–413.
Nylen, T.H., Fountain, A.G., Doran, P.T., 2004. Climatology of katabatic winds in the McMurdo dry valleys, southern Victoria Land, Antarctica. J. Geophys. Res. 109, D03114.
Peters, N.A., Huntington, K.W., Hoke, G.D., 2012. Hot or not? Impact of seasonally variable soil carbonate formation on paleotemperature and O-isotope records from clumped isotope thermometry. Earth Planet. Sci. Lett. 361, 208–218.
Quade, J., Breecker, D.O., Daeron, M., Eiler, J., 2011. The paleoaltimetry of Tibet: an isotopic perspective. Am. J. Sci. 311, 77–115.
Raymo, M.E., 1994. The initiation of northern hemisphere glaciation. Annu. Rev. Earth Planet. Sci. 22, 353–383.
Rowley, D.B., Garzione, C.N., 2007. Stable isotope-based paleoaltimetry. Annu. Rev. Earth Planet. Sci. 35, 463–508.
Schäfer, J.M., Ivy-Ochs, S., Wieler, R., Leya, I., Baur, H., Denton, G.H., Schlüchter, C., 1999. Cosmogenic noble gas studies in the oldest landscape on earth: surface exposure ages of the Dry Valleys, Antarctica. Earth Planet. Sci. Lett. 167, 215–226.
Schaller, M., Ehlers, T.A., Blum, J.D., Kallenberg, M.A., 2009. Quantifying glacial moraine age, denudation, and soil mixing with cosmogenic nuclide depth profiles. J. Geophys. Res. 114, F01012.
Shakun, J.D., Clark, P.U., He, F., Marcott, S.A., Mix, A.C., Liu, Z., Otto-Bliesner, B., Schmittner, A., Bard, E., 2012. Global warming preceded by increasing carbon dioxide concentrations during the last deglaciation. Nature 484, 49–54.
Shea, E.K., Weiss, B.P., Cassata, W.S., Shuster, D.L., Tikoo, S.M., Gattacceca, J., Grove, T.L., Fuller, M.D., 2012. A long-lived lunar core dynamo. Science 335, 453–456.
Shuster, D.L., Balco, G., Cassata, W.S., Fernandes, V.A., Garrick-Bethell, I., Weiss, B.P., 2010. A record of impacts preserved in the lunar regolith. Earth Planet. Sci. Lett. 290, 155–165.
Shuster, D.L., Farley, K.A., 2005. Diffusion kinetics of proton-induced ^{21}Ne, ^{3}He, and ^{4}He in quartz. Geochim. Cosmochim. Acta 69, 2349–2359.
Stone, J.O., 2000. Air pressure and cosmogenic isotope production. J. Geophys. Res. 105, 753–759.
Stone, J.O., Balco, G.A., Sugden, D.E., Caffee, M.W., Sass, L.C., Cowdery, S.G., Siddoway, C., 2003. Holocene deglaciation of Marie Byrd Land, West Antarctica. Science 299, 99–102.
Suavet, C., Weiss, B.P., Cassata, W.S., Shuster, D.L., Gattacceca, J., Chan, L., Garrick-Bethell, I., Head, J.W., Grove, T.L., Fuller, M.D., 2013. Persistence and origin of the lunar core dynamo. Proc. Natl. Acad. Sci. USA 110, 8453–8458.
Tremblay, M.M., Shuster, D.L., Balco, G., 2013. Quantifying the open-system behavior of cosmogenic noble gases in quartz. Mineral. Mag. 77, 2297–2370.
Trull, T., Brown, E., Marty, B., Raisbeck, G., Yiou, F., 1995. Cosmogenic ^{10}Be and ^{3}He accumulation in Pleistocene beach terraces in Death Valley, California, USA: implications for cosmic-ray exposure dating of young surfaces in hot climates. Chem. Geol. 119, 191–207.
Trull, T.W., Kurz, M.D., Jenkins, W.J., 1991. Diffusion of cosmogenic ^{3}He in olivine and quartz: implications for surface exposure dating. Earth Planet. Sci. Lett. 103, 241–256.
Vermeesch, P., Baur, H., Heber, V.S., Kober, F., Oberholzer, P., Schaefer, J.M., Schlüchter, C., Strasky, S., Wieler, R., 2009. Cosmogenic ^{3}He and ^{21}Ne measured in quartz targets after one year of exposure in the Swiss Alps. Earth Planet. Sci. Lett. 284, 417–425.
Wolf, R.A., Farley, K.A., Kass, D.M., 1998. Modeling of the temperature sensitivity of the apatite (U–Th)/He thermochronometer. Chem. Geol. 148, 105–114.